Draft version January 16, 2007
Preprint typeset using LaTeX style emulateapj v. 11/12/01

CONSTRAINTS ON HOLOGRAPHIC DARK ENERGY FROM LATEST SUPERNOVAE, GALAXY CLUSTERING, AND COSMIC MICROWAVE BACKGROUND ANISOTROPY OBSERVATIONS

Xin Zhang[1,2] and Feng-Quan Wu[1]

Draft version January 16, 2007

ABSTRACT

The holographic dark energy model is proposed by Li as an attempt for probing the nature of dark energy within the framework of quantum gravity. The main characteristic of holographic dark energy is governed by a numerical parameter c in the model. The parameter c can only be determined by observations. Thus, in order to characterize the evolving feature of dark energy and to predict the fate of the universe, it is of extraordinary importance to constrain the parameter c by using the currently available observational data. In this paper, we derive constraints on the holographic dark energy model from the latest observational data including the gold sample of 182 Type Ia supernovae (SNIa), the shift parameter of the cosmic microwave background (CMB) given by the three-year *Wilkinson Microwave Anisotropy Probe* (*WMAP*) observations, and the baryon acoustic oscillation (BAO) measurement from the Sloan Digital Sky Survey (SDSS). The joint analysis gives the fit results in 1-σ: $c = 0.91^{+0.26}_{-0.18}$ and $\Omega_{\rm m0} = 0.29 \pm 0.03$. That is to say, though the possibility of $c < 1$ is more favored, the possibility of $c > 1$ can not be excluded in one-sigma error range, which is somewhat different from the result derived from previous investigations using earlier data. So, according to the new data, the evidence for the quintom feature in the holographic dark energy model is not as strong as before.

Subject headings: cosmology: theory

1. INTRODUCTION

Observations of Type Ia supernovae (SNIa) indicate that the universe is experiencing an accelerating expansion at the present stage (Riess et al. 1998; Perlmutter et al. 1999). This cosmic acceleration has also been confirmed by observations of large scale structure (LSS; Tegmark et al. 2004; Abazajian et al. 2004) and measurements of the cosmic microwave background (CMB) anisotropy (Spergel et al. 2003; Bennett et al. 2003). The cause for this cosmic acceleration is usually referred to as "dark energy", a mysterious exotic matter with large enough negative pressure, whose energy density has been a dominative power of the universe (for reviews see e.g. Weinberg 1989; Sahni & Starobinsky 2000; Carroll 2001; Peebles & Ratra 2003; Padmanabhan 2003; Copeland et al. 2006). The astrophysical feature of dark energy is that it remains unclustered at all scales where gravitational clustering of baryons and nonbaryonic cold dark matter can be seen. Its gravity effect is shown as a repulsive force so as to make the expansion of the universe accelerate when its energy density becomes dominative power of the universe. The combined analysis of cosmological observations suggests that the universe is spatially flat, and consists of about 70% dark energy, 30% dust matter (cold dark matter plus baryons), and negligible radiation. Although we can affirm that the ultimate fate of the universe is determined by the feature of dark energy, the nature of dark energy as well as its cosmological origin remain enigmatic at present. However, we still can propose some candidates to interpret or describe the properties of dark energy. The most obvious theoretical candidate of dark energy is the cosmological constant λ (Einstein 1917) which always suffers from the "fine-tuning" and "cosmic coincidence" puzzles. Theorists have made lots of efforts to try to resolve the cosmological constant problem, but all these efforts were turned out to be unsuccessful. Numerous other candidates for dark energy have also been proposed in the literature, such as an evolving canonical scalar field (Peebles & Ratra 1988; Wetterich 1988; Caldwell et al. 1998; Zlatev et al. 1999; Zhang 2005a,b) usually referred to as quintessence, the phantom energy (Caldwell 2002; Caldwell et al. 2003) with an equation-of-state smaller than -1 violating the weak energy condition, the quintom energy (Feng et al. 2005; Guo et al. 2005; Zhang 2005c; Zhang et al. 2006; Zhang, Zhang & Liu 2006; Cai et al. 2007) with an equation-of-state evolving across -1, the hessence model (Wei et al. 2005; Wei & Cai 2005; Wei et al. 2006), the Chaplygin gas model (Kamenshchik et al. 2001; Bento et al. 2002; Zhang et al. 2006), and so forth.

Actually, the dark energy problem may be in principle a problem belongs to quantum gravity domain (Witten 2000). Another promising model for dark energy, the holographic dark energy model, was proposed by Li (2004) from some considerations of fundamental principle in the quantum gravity. It is well known that the holographic principle is an important result of the recent researches for exploring the quantum gravity or string theory ('t Hooft 1993; Susskind 1994). This principle is enlightened by investigations of the quantum property of black holes. Roughly speaking, in a quantum gravity system, the conventional local quantum field theory will break down. The reason is rather simple: For a quantum gravity system, the conventional local quantum field theory contains too many degrees of freedom, and such many degrees of freedom will lead to the formation of black hole so as to break down the effectiveness of the quantum field theory.

[1] National Astronomical Observatories, Chinese Academy of Sciences, Beijing 100012, People's Republic of China
[2] Institute of Theoretical Physics, Chinese Academy of Sciences, P.O.Box 2735, Beijing 100080, People's Republic of China

For an effective field theory in a box of size L, with UV cut-off Λ the entropy S scales extensively, $S \sim L^3\Lambda^3$. However, the peculiar thermodynamics of black hole (Bekenstein 1973, 1974, 1981, 1994; Hawking 1975, 1976) has led Bekenstein to postulate that the maximum entropy in a box of volume L^3 behaves nonextensively, growing only as the area of the box, i.e. there is a so-called Bekenstein entropy bound, $S \leq S_{BH} \equiv \pi M_{\rm Pl}^2 L^2$. This nonextensive scaling suggests that quantum field theory breaks down in large volume. To reconcile this breakdown with the success of local quantum field theory in describing observed particle phenomenology, Cohen et al. (1999) proposed a more restrictive bound – the energy bound. They pointed out that in quantum field theory a short distance (UV) cut-off is related to a long distance (IR) cut-off due to the limit set by forming a black hole. In other words, if the quantum zero-point energy density $\rho_{\rm vac}$ is relevant to a UV cut-off, the total energy of the whole system with size L should not exceed the mass of a black hole of the same size, thus we have $L^3\rho_{\rm vac} \leq LM_{\rm Pl}^2$. This means that the maximum entropy is in order of $S_{BH}^{3/4}$. When we take the whole universe into account, the vacuum energy related to this holographic principle ('t Hooft 1993; Susskind 1994) is viewed as dark energy, usually dubbed holographic dark energy (its density is denoted as $\rho_{\rm de}$ hereafter). The largest IR cut-off L is chosen by saturating the inequality so that we get the holographic dark energy density

$$\rho_{\rm de} = 3c^2 M_{\rm Pl}^2 L^{-2} \ , \tag{1}$$

where c is a numerical constant, and $M_{\rm Pl} \equiv 1/\sqrt{8\pi G}$ is the reduced Planck mass. If we take L as the size of the current universe, for instance the Hubble radius H^{-1}, then the dark energy density will be close to the observational result. However, Hsu (2004) pointed out that this yields a wrong equation of state for dark energy. Li (2004) subsequently proposed that the IR cut-off L should be taken as the size of the future event horizon

$$R_{\rm eh}(a) = a\int_t^\infty \frac{dt'}{a(t')} = a\int_a^\infty \frac{da'}{Ha'^2} \ . \tag{2}$$

Then the problem can be solved nicely and the holographic dark energy model can thus be constructed successfully. The holographic dark energy scenario may provide simultaneously natural solutions to both dark energy problems as demonstrated in Li (2004). For extensive studies on the holographic dark energy model see e.g. Huang & Li (2004); Enqvist & Sloth (2004); Ke & Li (2005); Huang & Li (2005); Zhang (2005d); Pavon & Zimdahl (2005); Wang et al. (2005); Kim et al. (2005); Nojiri & Odintsov (2006); Hu & Ling (2006); Zhang (2006a,b); Chen et al. (2006).

The holographic dark energy model has been tested and constrained by various astronomical observations, such as SNIa (Huang & Gong 2004), CMB (Enqvist et al. 2005; Shen et al. 2005; Kao et al. 2005), combination of SNIa, CMB and LSS (Zhang & Wu 2005), the X-ray gas mass fraction of galaxy clusters (Chang et al. 2006), and the differential ages of passively evolving galaxies (Yi & Zhang 2006). Recently, the three-year data of *Wilkinson Microwave Anisotropy Probe* (*WMAP*) observations (Spergel et al. 2006) were announced. Moreover, Riess et al. (2006) lately released the up-to-date 182 "gold" data of SNIa from various sources analyzed in a consistent and robust mannor with reduced calibration errors arising from systematics. This paper aims at placing new observational constraints on the holographic dark energy model by using the gold sample of 182 SNIa compiled by Riess et al. (2006), the CMB shift parameter derived from three-year *WMAP* observations (Wang & Mukherjee 2006), and the baryon acoustic oscillations detected in the large-scale correlation function of Sloan Digital Sky Survey (SDSS) luminous red galaxies (Eisenstein et al. 2005).

This paper is organized as follows: In section 2 we discuss the basic characteristics of the holographic dark energy model. In section 3, we perform constraints on the holographic dark energy model by using the up-to-date observational datasets. Finally, we give the concluding remarks in section 4.

2. THE MODEL OF HOLOGRAPHIC DARK ENERGY

In this section, we shall review the holographic dark energy model briefly and discuss the basic characteristics of this model. Now let us consider a spatially flat Friedmann-Robertson-Walker (FRW) universe with matter component $\rho_{\rm m}$ (including both baryon matter and cold dark matter) and holographic dark energy component $\rho_{\rm de}$, the Friedmann equation reads

$$3M_{\rm Pl}^2 H^2 = \rho_{\rm m} + \rho_{\rm de} \ , \tag{3}$$

or equivalently,

$$E(z) \equiv \frac{H(z)}{H_0} = \left(\frac{\Omega_{\rm m0}(1+z)^3}{1-\Omega_{\rm de}}\right)^{1/2} , \tag{4}$$

where $z = (1/a) - 1$ is the redshift of the universe. Note that we always assume spatial flatness throughout this paper as motivated by inflation. Combining the definition of the holographic dark energy (1) and the definition of the future event horizon (2), we derive

$$\int_a^\infty \frac{d\ln a'}{Ha'} = \frac{c}{Ha\sqrt{\Omega_{\rm de}}} \ . \tag{5}$$

We notice that the Friedmann equation (4) implies

$$\frac{1}{Ha} = \sqrt{a(1-\Omega_{\rm de})}\frac{1}{H_0\sqrt{\Omega_{\rm m0}}} \ . \tag{6}$$

Substituting (6) into (5), one obtains the following equation

$$\int_x^\infty e^{x'/2}\sqrt{1-\Omega_{\rm de}}dx' = ce^{x/2}\sqrt{\frac{1}{\Omega_{\rm de}}-1} \ , \tag{7}$$

where $x = \ln a$. Then taking derivative with respect to x in both sides of the above relation, we get easily the dynamics satisfied by the dark energy, i.e. the differential equation about the fractional density of dark energy,

$$\Omega'_{\rm de} = -(1+z)^{-1}\Omega_{\rm de}(1-\Omega_{\rm de})\left(1+\frac{2}{c}\sqrt{\Omega_{\rm de}}\right), \tag{8}$$

where the prime denotes the derivative with respect to the redshift z. This equation describes behavior of the holographic dark energy completely, and it can be solved exactly (Li 2004). From the energy conservation equation of the dark energy, the equation of state of the dark energy can be given (Li 2004)

$$w = -1 - \frac{1}{3}\frac{d\ln\rho_{\rm de}}{d\ln a} = -\frac{1}{3}(1+\frac{2}{c}\sqrt{\Omega_{\rm de}}) \ . \tag{9}$$

Note that the formula $\rho_{\rm de} = \frac{\Omega_{\rm de}}{1-\Omega_{\rm de}}\rho_{\rm m0}a^{-3}$ and the differential equation of $\Omega_{\rm de}$ (8) are used in the second equal

sign. It can be seen clearly that the equation of state of the holographic dark energy evolves dynamically and satisfies $-(1+2/c)/3 \leq w \leq -1/3$ due to $0 \leq \Omega_{\rm de} \leq 1$. Hence, we see clearly that when taking the holographic principle into account the vacuum energy becomes dynamically evolving dark energy.

The parameter c plays a significant role in this model. If one takes $c = 1$, the behavior of the holographic dark energy will be more and more like a cosmological constant with the expansion of the universe, such that ultimately the universe will enter the de Sitter phase in the far future. As is shown in Li (2004), if one puts the parameter $\Omega_{\rm de0} = 0.73$ into (9), then a definite prediction of this model, $w_0 = -0.903$, will be given. On the other hand, if $c < 1$, the holographic dark energy will exhibit appealing behavior that the equation of state crosses the "cosmological-constant boundary" (or "phantom divide") $w = -1$ during the evolution. This kind of dark energy is referred to as "quintom" (Feng et al. 2005) which is slightly favored by current observations, see e.g. Alam et al. (2004); Huterer & Cooray (2005); Zhao et al. (2005); Xia et al. (2006); Zhao et al. (2006a); Li et al. (2006); Gong & Wang (2006); Zhao et al. (2006b). If $c > 1$, the equation of state of dark energy will be always larger than -1 such that the universe avoids entering the de Sitter phase and the Big Rip phase. Hence, we see explicitly, the value of c is very important for the holographic dark energy model, which determines the feature of the holographic dark energy as well as the ultimate fate of the universe. For an illustrative example, see Figure 1 in Zhang & Wu (2005), in which the selected evolutions in different c for the equation of state of holographic dark energy are plotted. It is clear to see that the cases in $c \geq 1$ always evolve in the region of $w \geq -1$, whereas the case of $c < 1$ behaves as a quintom whose equation of state w crosses the cosmological constant boundary $w = -1$ during the evolution. It has been shown in previous analyses of observational data (Zhang & Wu 2005; Chang et al. 2006; Yi & Zhang 2006) that the holographic dark energy exhibits quintom-like behavior basically within statistical error one sigma.

3. CONSTRAINTS FROM LATEST SNIA, LSS, AND CMB OBSERVATIONS

In this section, we constrain the parameters in the holographic dark energy model and analyze the evolutionary behavior of holographic dark energy by using the latest observational data of SNIa combined with the information from CMB and LSS observations.

Recently, the up-to-date gold sample of SNIa consists of 182 data was compiled by Riess et al. (2006). It contains 119 points from the previous sample compiled in Riess et al. (2004) and 16 points with $0.46 < z < 1.39$ discovered recently (Riess et al. 2006) by the *Hubble Space Telescope* (*HST*). It also incorporates 47 points ($0.25 < z < 0.96$) from the first year release of the Supernova Legacy Survey (SNLS) sample (Astier et al. 2006) out of a total of 73 distant SNIa. Some previous gold data were excluded in Riess et al. (2006) due to highly uncertain color measurements, high extinction $A_V > 0.5$ and a redshift cut $z < 0.0233$, to avoid the influence of a possible local "Hubble Bubble", so as to define a high-confidence sample. The total gold sample spans a wide range of redshift $0.024 < z < 1.76$. For recent usages of the new sample, see e.g. Barger et al. (2006); Alam et al. (2006); Li et al. (2006); Gong & Wang (2006); Zhang, Zhang & Liu (2006); Nesseris & Perivolaropoulos (2006); Zhao et al. (2006b); Wei et al. (2006). We shall analyze the holographic dark energy model in the light of the new gold sample of SNIa.

The SNIa observations directly measure the apparent magnitude m of a supernova and its redshift z. The apparent magnitude m is related to the luminosity distance d_L of the supernova through

$$m(z) = M + 5\log_{10}(d_L(z)/{\rm Mpc}) + 25 \ , \qquad (10)$$

where M is the absolute magnitude which is believed to be constant for all Type Ia supernovae, and the luminosity distance-redshift relation is

$$d_L(z) = \left(\frac{\mathcal{L}}{4\pi\mathcal{F}}\right)^{1/2} = H_0^{-1}(1+z)\int_0^z \frac{dz'}{E(z')} \ , \qquad (11)$$

where $\mathcal{L}$ is the absolute luminosity which is a known value for the standard candle SNIa, $\mathcal{F}$ is the measured flux, H_0^{-1} (here we use the natural unit, namely the speed of light is defined to be 1) represents the Hubble distance with value $H_0^{-1} = 2997.9h^{-1}$ Mpc, and $E(z) = H(z)/H_0$ is expressed in equation (4). Note that the dynamical behavior of $\Omega_{\rm de}$ is governed by differential equation (8). In order to place constraints on the holographic dark energy model, we perform χ^2 statistics for the model parameters $(c, \Omega_{\rm m0})$ and the present Hubble parameter H_0. For the SNIa analysis, we have

$$\chi^2_{\rm SN} = \sum_{i=1}^{182} \frac{[\mu_{\rm obs}(z_i) - \mu_{\rm th}(z_i)]^2}{\sigma_i^2} \ , \qquad (12)$$

where the extinction-corrected distance moduli $\mu(z)$ is defined as $\mu(z) = m(z) - M$, and σ_i is the total uncertainty in the observation. The likelihood $\mathcal{L} \propto e^{-\chi^2/2}$ if the measurement errors are Gaussian. The best-fit for the analysis of gold sample of 182 SNIa happens at $c = 0.37$, $\Omega_{\rm m0} = 0.43$, and $h = 0.64$, with $\chi^2_{\rm min} = 156.60$. The gold sample is illustrated on a residual Hubble diagram with respect to our best-fit universe in Figure 1. Since we concentrate on the model parameters $(c, \Omega_{\rm m0})$, we need to marginalize over the Hubble parameter H_0. Note that marginalizing over H_0 is equivalent to evaluating χ^2 at its minimum with respect to H_0 (Barris et al. 2004). We marginalize over the nuisance parameter h and show the probability contours at 68.3%, 95.4%, and 99.7% confidence levels for c vs. $\Omega_{\rm m0}$ in Figure 2, from the constraints of gold sample of SNIa, as purple dot-dashed contours. The 1 σ fit values for the model parameters are: $c = 0.37^{+0.56}_{-0.21}$ and $\Omega_{\rm m0} = 0.43^{+0.08}_{-0.14}$. We see that the parameter c in 1 σ range, $0.16 < c < 0.93$, is smaller than 1, making the holographic dark energy behave as quintom with equation-of-state evolving across $w = -1$, according to this analysis.

On the other hand, the above analysis shows that the SNIa data alone seem not sufficient to constrain the holographic dark energy model strictly. The confidence region of $c-\Omega_{\rm m0}$ plane is rather large, especially for the parameter c. Moreover, it is remarkable that the best fit value of $\Omega_{\rm m0}$ of this model is evidently larger than that of the ΛCDM model. For comparison, we refer to the *WMAP* result

for $\Omega_{\rm m0}$ in ΛCDM model: $\Omega_{\rm m0}=0.24^{+0.03}_{-0.04}$ (Spergel et al. 2006). As has been elucidated in Zhang & Wu (2005) that for the holographic dark energy the fit of SNIa data is very sensitive to the Hubble parameter H_0, so it is very important to find other observational quantities irrelevant to H_0 as a complement to SNIa data. Fortunately, such suitable data can be found in the probes of CMB and LSS.

For the CMB data, we use the CMB shift parameter. The CMB shift parameter R is perhaps the least model-independent parameter that can be extracted from CMB data. The shift parameter R is given by (Bond et al. 1997)

$$R\equiv\Omega_{\rm m0}^{1/2}\int_0^{z_{\rm CMB}}\frac{dz'}{E(z')}, \tag{13}$$

where $z_{\rm CMB}=1089$ is the redshift of recombination. The value of the shift parameter R can be determined by three-year integrated *WMAP* analysis (Spergel et al. 2006), and has been updated by Wang & Mukherjee (2006) to be 1.70 ± 0.03 independent of the dark energy model. For the LSS data, we use the measurement of the BAO peak in the distribution of SDSS luminous red galaxies (LRGs). The SDSS BAO measurement (Eisenstein et al. 2005) gives $A=0.469(n_s/0.98)^{-0.35}\pm0.017$ (independent of a dark energy model) at $z_{\rm BAO}=0.35$, where A is defined as

$$A\equiv\Omega_{\rm m0}^{1/2}E(z_{\rm BAO})^{-1/3}\left[\frac{1}{z_{\rm BAO}}\int_0^{z_{\rm BAO}}\frac{dz'}{E(z')}\right]^{2/3}. \tag{14}$$

Here the scalar spectral index is taken to be $n_s=0.95$ as measured by the three-year *WMAP* data (Spergel et al. 2006). We notice that both R and A are independent of H_0; thus these quantities can provide robust constraint as complement to SNIa data on the holographic dark energy model.

We now perform a combined analysis of SNIa, CMB, and LSS on the constraints of the holographic dark energy model. We use the χ^2 statistics

$$\chi^2=\chi^2_{\rm SN}+\chi^2_{\rm CMB}+\chi^2_{\rm LSS}\ , \tag{15}$$

where $\chi^2_{\rm SN}$ is given by equation (12) for SNIa statistics, $\chi^2_{\rm CMB}=[(R-R_{\rm obs})/\sigma_R]^2$ and $\chi^2_{\rm LSS}=[(A-A_{\rm obs})/\sigma_A]^2$ are contributions from CMB and LSS data, respectively. The main results are shown in Figure 2. In this figure, we show the contours of 68.3%, 95.4%, and 99.7% confidence levels in the $c-\Omega_{\rm m0}$ plane. The constraints from the shift parameter R in CMB are illustrated by the red solid contours; the constraints from the parameter A in BAO are illustrated by green dashed contours; the joint constraints from SNIa+CMB+LSS are shown as shaded contours. It is clear to see that the combined analysis of SNIa, CMB and LSS data provides a fairly tight constraint on the holographic dark energy model, comparing to the constraint from the SNIa gold sample alone. The fit values for the model parameters with 1-σ errors are $c=0.91^{+0.26}_{-0.18}$ and $\Omega_{\rm m0}=0.29\pm0.03$ with $\chi^2_{\rm min}=158.97$. For comparison, the fit results from the SNIa gold sample alone and from the combination of SNIa, CMB and LSS are shown in Table 1. We also show the best-fit case of SNIa+CMB+LSS analysis on the residual Hubble diagram with respect to the best-fit case of SNIa alone analysis in Figure 1. We see clearly that in the joint analysis the derived value for matter density $\Omega_{\rm m0}$ is very reasonable. In addition, it should be emphasized that what is of importance for this model is the determination of the value of c. In figure 3 we plot the 1-dimensional likelihood function for c, marginalizing over the other parameters. We notice that the best-fit value of c in this analysis is enhanced to around 0.91. Intriguingly, the range of c in 1-σ error, $0.73<c<1.17$, is not capable of ruling out the probability of $c>1$; this conclusion is somewhat different from those derived from previous investigations using earlier data. In previous work, for instance, Zhang & Wu (2005) and Chang et al. (2006), the 1-σ range of c obtained can basically exclude the probability of $c>1$ giving rise to the quintessence-like behavior, supporting the quintom-like behavior evidently. Though the present result (in 1-σ error range) from the analysis of the up-to-date observational data does not support the quintom-like feature as strongly as before, the best-fit value ($c=0.91$) still exhibits the holographic quintom characteristic.

Another problem of concern is that both the SNIa alone analysis and the SNIa+CMB+LSS joint analysis predict a low value of dimensionless Hubble constant h. For the Hubble constant, one of the most reliable results comes from the *Hubble Space Telescope* Key Project (Freeman et al. 2001). The group of Freeman has used the empirical period-luminosity relations for Cepheid variable stars to obtain distances to 31 galaxies, and calibrated a number of secondary distance indicators measured over distances of 400 to 600 Mpc. The result they obtained is $h=0.72\pm0.08$. It is remarkable that, intriguingly, this result is in such good agreement with the result derived from the *WMAP* CMB measurements, $h=0.73^{+0.03}_{-0.04}$ (it should be pointed out that this result is derived from a flat ΛCDM model assumption; Spergel et al. 2006).

In the follows we shall incorporate the *HST* Hubble constant result into the SNIa+CMB+LSS data fitting. First, we add the *HST* term, $\chi^2_{HST}=[(h-0.72)/0.08]^2$, to the total χ^2. The results we derived are shown in Firgure 4, the 1, 2 and 3 σ contours of confidence levels in $c-\Omega_{\rm m0}$ plane. The fit values for model parameters with one-sigma errors are $c=0.91^{+0.23}_{-0.19}$ and $\Omega_{\rm m0}=0.29\pm0.03$, which are almost the same as the results from without *HST* data. So, we next take another way of incorporating the *HST* prior, $0.64<h<0.80$, into account, in the data analysis. When considering this prior, the confidence level contours get shrinkage and left-shift in the $c-\Omega_{\rm m0}$ parameter-plane, as shown in Figure 5. In this case the fit values for model parameters with one-sigma errors are $c=0.82^{+0.11}_{-0.13}$ and $\Omega_{\rm m0}=0.28^{+0.03}_{-0.02}$. We see that the holographic dark energy features quintom dark energy within one-sigma range in this case. Furthermore, we also consider a strong *HST* prior, fixing $h=0.72$, in order to see how strongly biased constraints can be derived from a factitious prior on h. We plot the results of this case in Figure 6. The fit values for model parameters with one-sigma errors are $c=0.42\pm0.05$ and $\Omega_{\rm m0}=0.24^{+0.02}_{-0.03}$. We find that the shrinkage and the left-shift for the confidence level contours become more evident. For illustrating the cosmological consequences led by the observational constraints, we show the evolution cases of the equation-of-state parameter $w(z)$ and the deceleration parameter $q(z)$ according to some best-fit values of parameters of the holographic dark energy model in Figure 7 and 8. The quintom feature with $w=-1$ crossing characteristic for the holographic dark energy model can be easily seen.

TABLE 1
CONSTRAINTS FROM OBSERVATIONAL DATA

Parameter/Quantity	SNIa gold sample alone	SNIa+CMB+LSS
c	$0.37^{+0.56}_{-0.21}$	$0.91^{+0.26}_{-0.18}$
$\Omega_{\rm m0}$	$0.43^{+0.08}_{-0.14}$	$0.29^{+0.03}_{-0.03}$
h	0.64	0.63
$\chi^2_{\rm min}$	156.60	158.97

Note. — The fit values of c and $\Omega_{\rm m0}$ are given in 1-σ errors; the fit value of h is given at best-fit case; the value of $\chi^2_{\rm min}$ is also for best-fit.

4. CONCLUDING REMARKS

The cosmic acceleration observed by distance-redshift relation measurement of SNIa strongly supports the existence of dark energy. The fantastic physical property of dark energy not only drives the current cosmic acceleration, but also determines the ultimate fate of the universe. However, hitherto, the nature of dark energy as well as its cosmological origin still remain enigmatic for us. Though the underlying theory of dark energy is still far beyond our knowledge, it is guessed that the quantum gravity theory shall play a significant role in resolving the dark energy enigma. The holographic dark energy model is proposed as an attempt for probing the nature of dark energy within the framework of quantum gravity, i.e. it is based upon an important fundamental principle of quantum gravity — holographic principle, so it possesses some significant features of an underlying theory of dark energy. The main characteristic of holographic dark energy is governed by a numerical parameter c in the model. This parameter, c, can only be determined by observations. Hence, in order to characterize the evolving feature of dark energy and to predict the fate of the universe, it is of extraordinary importance to constrain the parameter c by using the currently available observational data. In this paper, we have analyzed the holographic dark energy model by using the up-to-date gold SNIa sample, combined with the CMB and LSS data. Since the SNIa data are sensitive to the Hubble constant H_0, while the shift parameter in CMB and the parameter in the BAO are irrelevant to the Hubble parameter, the combination of these datasets leads to strong constraints on the model parameters, as shown in Figure 2. The joint analysis indicates that, though the possibility of $c < 1$ is more favored, the possibility of $c > 1$ can not be excluded in one-sigma error range, which is somewhat different from the result derived from previous investigations using earlier data (such as Zhang & Wu 2005, in which the result of $c < 1$ is basically favored in 1-σ range). That is to say, according to the new data, the evidence for the quintom feature in the holographic dark energy model is not as strong as before. However, when considering the *HST* prior, $0.64 < h < 0.80$, the quintom-like behavior can be supported in one-sigma error range, as shown in Figure 5. On the whole, the current observational data have no ability to constrain the parameters in the holographic dark energy model on a high precision level. We expect that the future high-precision observations such as the SuperNova/Acceleration Project (SNAP) will be capable of determining the value of c exactly and thus revealing the property of the holographic dark energy.

ACKNOWLEDGEMENTS

We would like to thank Qing-Guo Huang, Miao Li, and Hao Wei for helpful discussions. This work was partially supported by the National Natural Science Foundation of China. XZ also thanks the financial support from China Postdoctoral Science Foundation.

REFERENCES

't Hooft, G., 1993, preprint (gr-qc/9310026)
Abazajian, K., *et al.*, 2004 ApJ, 128, 502
Alam, U., Sahni, V., & Starobinsky, A. A., 2004, J. Cosmology Astropart. Phys., 06, 008
Alam, U., Sahni, V., & Starobinsky, A. A., 2006, preprint (astro-ph/0612381)
Astier, P., et al. 2006, A&A, 447, 31
Barger, V., Gao, Y., & Marfatia, D., 2006, preprint (astro-ph/0611775)
Barris, B. J., et al. 2004, ApJ, 602, 571
Bekenstein, J. D., 1973, Phys. Rev. D, 7, 2333
Bekenstein, J. D., 1974, Phys. Rev. D, 9, 3292
Bekenstein, J. D., 1981, Phys. Rev. D, 23, 287
Bekenstein, J. D., 1981, Phys. Rev. D, 49, 1912
Bennett, C. L., et al. 2003, ApJS, 148, 1
Bento, M. C., Bertolami, O., & Sen, A. A., 2002, Phys. Rev. D, 66, 043507
Bond, J. R., Efstathiou, G., & Tegmark, M., 1997, MNRAS, 291, L33
Cai, Y. F., et al. 2007, preprint (hep-th/0701016)
Caldwell, R. R., Dave R., & Steinhardt, P. J., 1998, Phys. Rev. Lett., 80, 1582
Caldwell, R. R., 2002, Phys. Lett. B 545, 23
Caldwell, R. R., Kamionkowski, M., & Weinberg, N. N., 2003, Phys. Rev. Lett., 91, 071301
Carroll, S. M., 2001, Living Rev. Relativity, 4, 1
Chang, Z., Wu, F. Q., & Zhang, X., 2006, Phys. Lett. B, 633, 14
Chen, B., Li, M., & Wang, Y., 2006, preprint (astro-ph/0611623)
Cohen, A. G., Kaplan, D. B., & Nelson, A. E., 1999, Phys. Rev. Lett., 82, 4971
Copeland, E. J., Sami, M., & Tsujikawa, S., 2006, preprint (hep-th/0603057)
Einstein, A., 1917, Sitzungsber. K. Preuss. Akad. Wiss., 142 [*The Principle of Relativity* (Dover, New York, 1952), p. 177].
Eisenstein, D. J., et al. 2005, ApJ, 633, 560

Enqvist, K., & Sloth, M. S., 2004, Phys. Rev. Lett., 93, 221302
Enqvist, K., Hannestad, S., & Sloth, M. S., 2005, J. Cosmology Astropart. Phys., 02, 004
Feng, B., Wang, X. L., & Zhang, X. M., 2005, Phys. Lett. B 607, 35
Freeman, W. L., et al. 2001, ApJ, 553, 47
Gong, Y., & Wang, A., 2006, preprint (astro-ph/0612196)
Guo, Z. K., Piao, Y. S., Zhang, X. M., & Zhang, Y. Z., Phys. Lett. B 608, 177
Hawking, S. W., 1975, Commun. Math. Phys., 43, 199
Hawking, S. W., 1976, Phys. Rev. D, 13, 191
Hsu, S. D. H., 2004, Phys. Lett. B, 594, 13
Hu, B., & Ling, Y., 2006, Phys. Rev. D, 73, 123510
Huang, Q. G., & Gong, Y. G., 2004, J. Cosmology Astropart. Phys., 08, 006
Huang, Q. G., & Li, M., 2004, J. Cosmology Astropart. Phys., 08, 013
Huang, Q. G., & Li, M., 2005, J. Cosmology Astropart. Phys., 03, 001
Huterer, D., & Cooray, A., 2005, Phys. Rev. D, 71, 023506
Kamenshchik, A. Y., Moschella, U. & Pasquier, V., 2001, Phys. Lett. B, 511, 265
Kao, H. C., Lee, W. L., & Lin, F. L., 2005, Phys. Rev. D, 71, 123518
Ke, K., & Li, M., 2005, Phys. Lett. B, 606, 173
Kim, H., Lee, H. W., & Myung, Y. S., 2005, Phys. Lett. B 632, 605
Li, M., 2004, Phys. Lett. B, 603, 1
Li, H., et al. 2006, preprint (astro-ph/0612060)
Nesseris, S., & Perivolaropoulos, L., 2006, preprint (astro-ph/0612653)
Nojiri, S., & Odintsov, S. D., 2006, Gen. Rel. Grav. 38, 1285
Padmanabhan, T., 2003, Phys. Rep. 380, 235
Pavon, D., & Zimdahl, W., 2005, Phys. Lett. B, 628, 206
Peebles, P. J. E., & Ratra, B., 1988, ApJ, 325, 17
Peebles, P. J. E., & Ratra, B., 2003, Rev. Mod. Phys., 75, 559
Perlmutter, S. *et al.*, 1999, ApJ, 517, 565
Riess, A. G, *et al.*, 1998, Astron. J., 116, 1009
Riess, A. G, *et al.*, 2004, ApJ, 607, 665
Riess, A. G., et al. 2006, ApJ, accepted (astro-ph/0611572)
Shen, J., Wang, B., Abdalla, E., & Su, R. K., 2005, Phys. Lett. B, 609, 200
Spergel, D.N., *et al.*, 2003, ApJS, 148, 175
Spergel, D. N., et al. 2006, ApJ, submitted (astro-ph/0603449)
Sahni, V., & Starobinsky, A. A., 2000, Int. J. Mod. Phys. D, 9, 373
Susskind, L., 1994, J. Math. Phys. 36, 6377
Tegmark, M., *et al.*, 2004, Phys. Rev. D, 69, 103501
Wang, Y., & Mukherjee, P., 2006, ApJ, 650, 1
Wang, B., Gong, B., & Abdalla, E., 2005, Phys. Lett. B 624, 141
Wei, H., Cai, R. G., & Zeng, D. F., 2005, Class. Quant. Grav., 22, 3189
Wei, H., & Cai, R. G., Phys. Rev. D, 72, 123507
Wei, H., Tang, N., & Zhang, S. N., 2006, preprint (astro-ph/0612746)
Weinberg, S., 1989, Rev. Mod. Phys., 61, 1
Wetterich, C., 1988, Nucl. Phys. B, 302 668
Witten, E., 2000, preprint (hep-ph/0002297)
Xia, J. Q., Zhao, G. B., Feng, B., Li, H., & Zhang, X. M., 2006, Phys. Rev. D, 73, 063521
Yi, Z. L., & Zhang, T. J., 2006, Mod. Phys. Lett. A, 22, 41
Zhang, J., Zhang, X., & Liu, H., 2006, preprint (astro-ph/0612642)
Zhang, X., 2005a, Mod. Phys. Lett. A 20, 2575
Zhang, X., 2005b, Phys. Lett. B 611, 1
Zhang, X., 2005c, Commun. Theor. Phys. 44, 762
Zhang, X., 2005d, Int. J. Mod. Phys. D, 14, 1597
Zhang, X., 2006a, preprint (astro-ph/0604484)
Zhang, X., 2006b, Phys. Rev. D, 74, 103505
Zhang, X., & Wu, F. Q., 2005, Phys. Rev. D, 72, 043524
Zhang, X., Wu, F. Q., & Zhang, J., 2006, J. Cosmology Astropart. Phys., 01, 003
Zhang, X. F., Li, H., Piao, Y. S., & Zhang, X. M., 2006, Mod. Phys. Lett. A, 21, 231
Zhao, G. B., Xia, J. Q., Li, M. Z., Feng, B., & Zhang, X. M., 2005, Phys. Rev. D, 72, 123515
Zhao, G. B., Xia, J. Q., Feng, B., & Zhang, X. M., 2006a, preprint (astro-ph/0603621)
Zhao, G. B., et al. 2006b, preprint (astro-ph/0612728)
Zlatev, I., Wang L. M., & Steinhardt, P. J., 1999, Phys. Rev. Lett., 82, 896

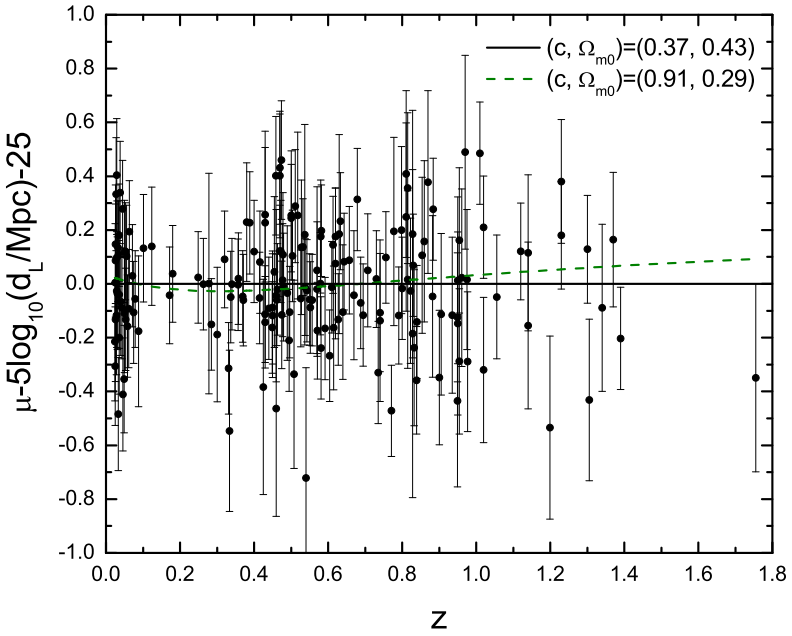

FIG. 1.— Gold sample of 182 SNIa residual Hubble diagram comparing holographic dark energy model with best-fit values for parameters. The black solid line represents the best-fit for SNIa alone analysis with $(c,\ \Omega_{\rm mo}) = (0.37,\ 0.43)$; The green dashed line represents the best-fit for SNIa+CMB+LSS joint analysis with $(c,\ \Omega_{\rm mo}) = (0.91,\ 0.29)$. Data and model are shown relative to the case of $(c,\ \Omega_{\rm mo}) = (0.37,\ 0.43)$.

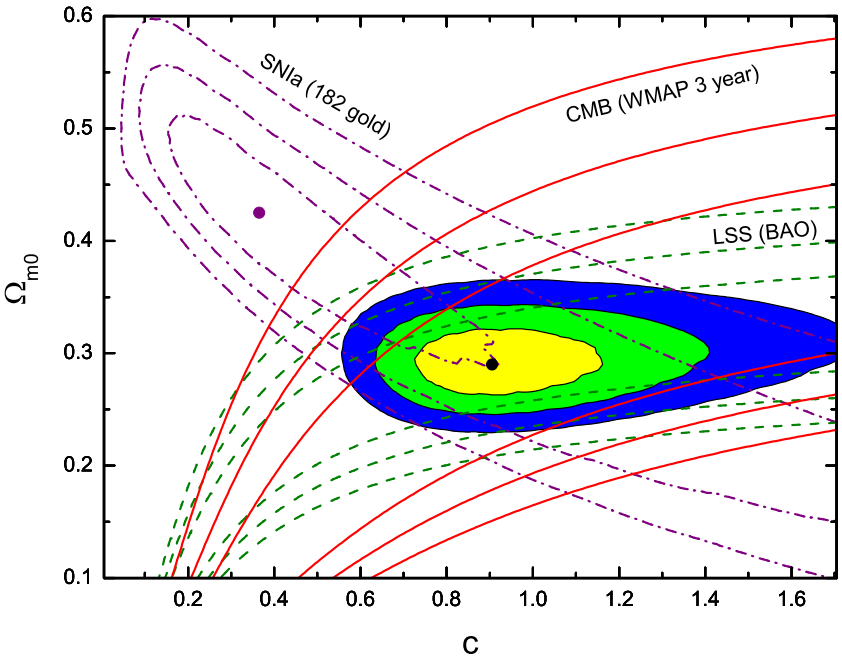

FIG. 2.— Probability contours at 68.3%, 95.4%, and 99.7% confidence levels in $(c,\ \Omega_{\rm m0})$-plane, for the holographic dark energy model, from the gold sample of SNIa data (purple dot-dashed contours), from the shift parameter R in CMB (red solid contours), from the parameter A in BAO found in the SDSS (green dashed contours), and from the combination of the three databases (shaded contours). The points show the best-fit cases for SNIa alone analysis and for SNIa+CMB+LSS joint analysis, respectively.

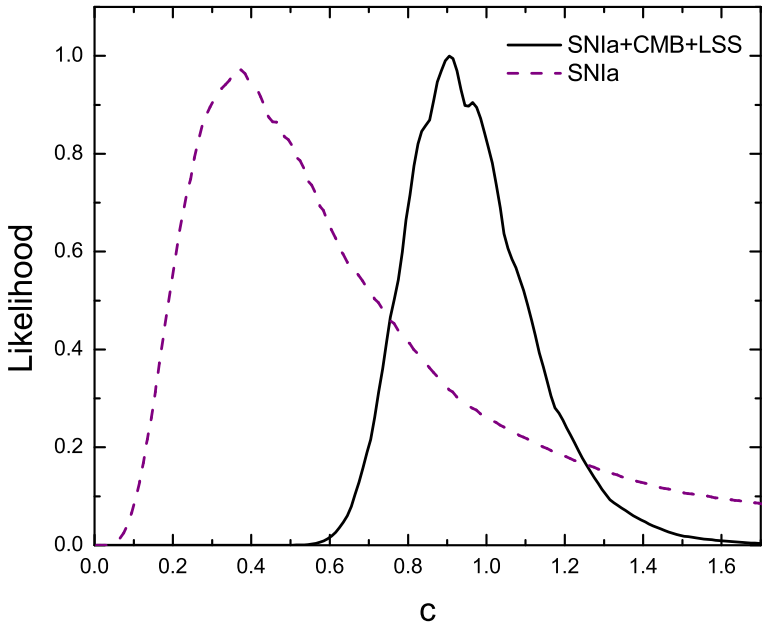

FIG. 3.— Probability distribution of parameter c for the fits of SNIa alone and SNIa+CMB+LSS.

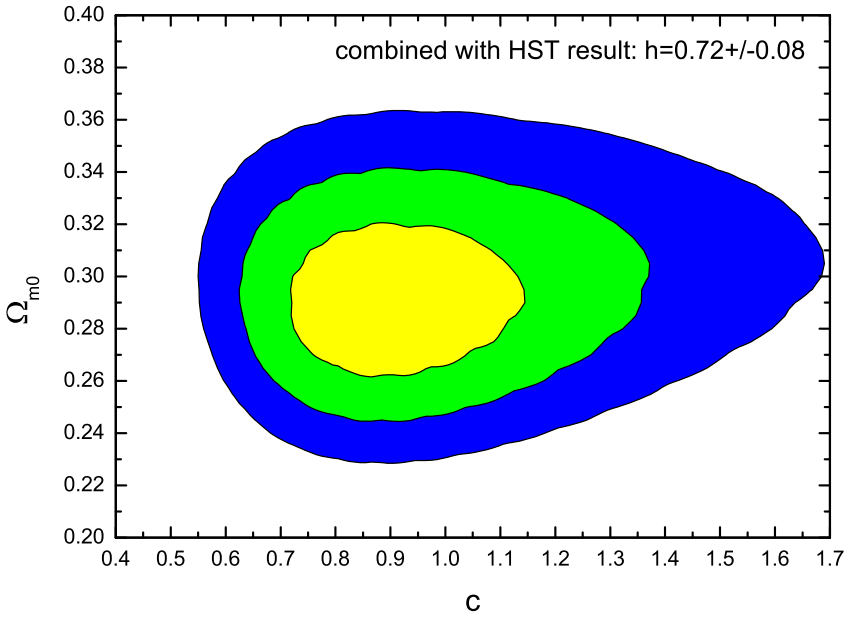

FIG. 4.— Probability contours at 68.3%, 95.4%, and 99.7% confidence levels in (c, $\Omega_{\rm m0}$)-plane, for the holographic dark energy model, from the constraints of the combination of SNIa, CMB and LSS. In this analysis, the *HST* prior $h = 0.72 \pm 0.08$ is also considered by adding a term $\chi^2_{HST} = [(h-0.72)/0.08]^2$ to the total χ^2. The fit values for model parameters with one-sigma errors are $c = 0.91^{+0.23}_{-0.19}$ and $\Omega_{\rm m0} = 0.29 \pm 0.03$, which are almost the same as the results without prior, see Figure 2.

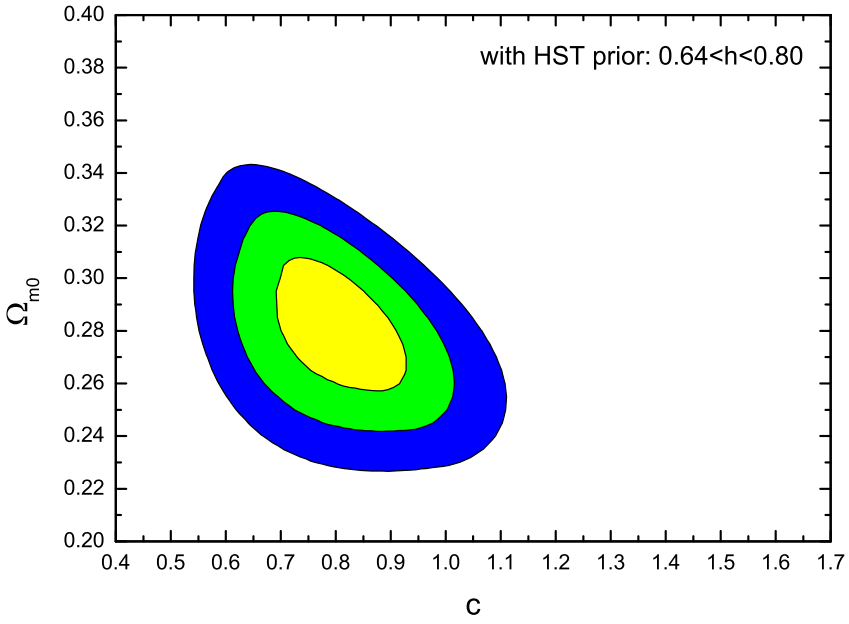

FIG. 5.— Probability contours at 68.3%, 95.4%, and 99.7% confidence levels in (c, $\Omega_{\rm m0}$)-plane, for the holographic dark energy model, from the constraints of the combination of SNIa, CMB and LSS, also with *HST* prior $0.64 < h < 0.80$. The fit values for model parameters with one-sigma errors are $c = 0.82^{+0.11}_{-0.13}$ and $\Omega_{\rm m0} = 0.28^{+0.03}_{-0.02}$.

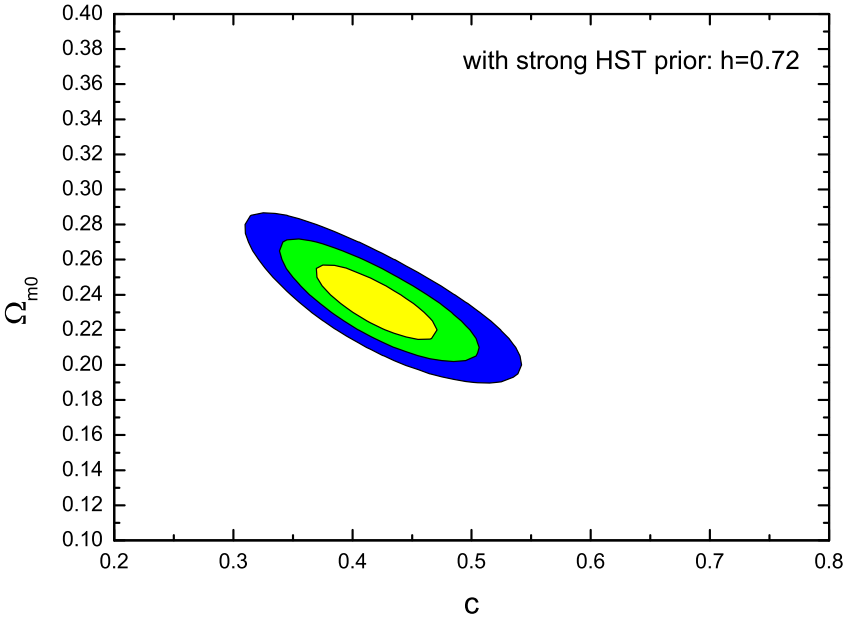

FIG. 6.— Same as Figure 5, but with strong-*HST* prior $h = 0.72$. The fit values for model parameters with one-sigma errors are $c = 0.42 \pm 0.05$ and $\Omega_{\rm m0} = 0.24^{+0.02}_{-0.03}$.

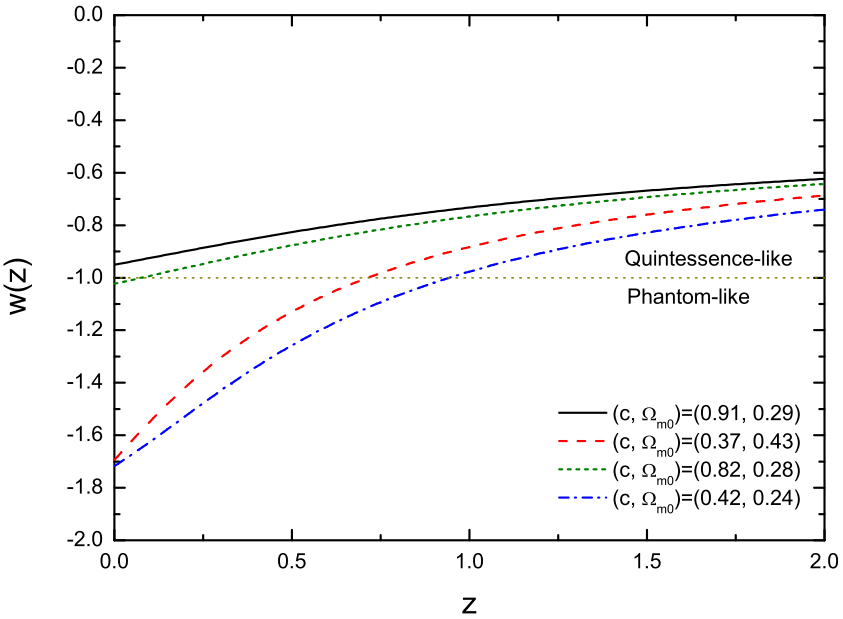

FIG. 7.— The equation-of-state parameter of dark energy w versus redshift z, from some best-fit values of the holographic dark energy model.

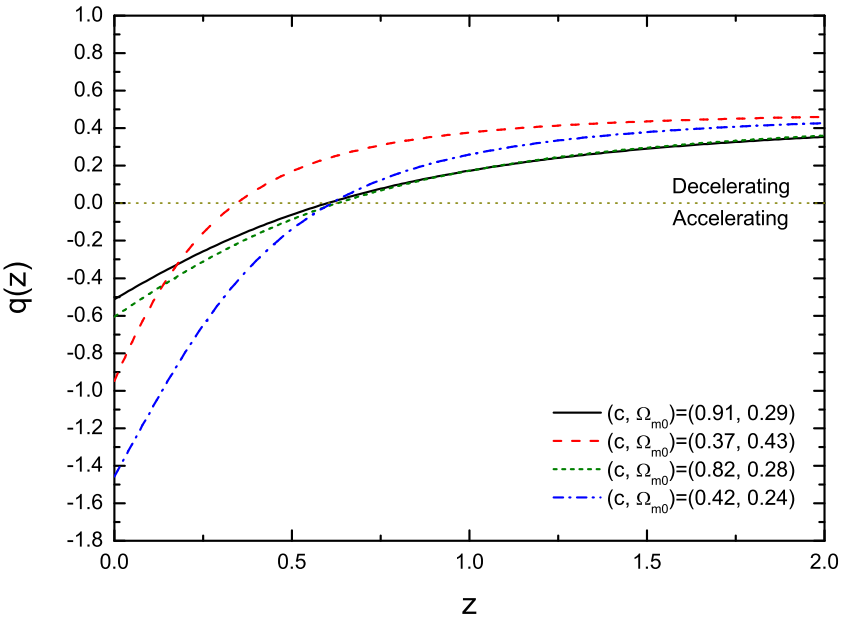

FIG. 8.— Deceleration parameter q versus redshift z, from some best-fit values of the holographic dark energy model.